Casimir-Polder interaction between an atom and a small magnetodielectric sphere

Agnes Sambale
Theoretisch-Physikalisches Institut, Friedrich-Schiller-Universität Jena, Max-Wien-Platz 1, D-07743 Jena, Germany

Stefan Yoshi Buhmann and Stefan Scheel
Quantum Optics and Laser Science, Blackett Laboratory, Imperial College London, Prince Consort Road, London SW7 2BW, United Kingdom

(Received 27 August 2009; published 28 January 2010)

On the basis of macroscopic quantum electrodynamics and point-scattering techniques, we derive a closed expression for the Casimir-Polder force between a ground-state atom and a small magnetodielectric sphere in an arbitrary environment. To allow for the presence of both bodies and media, local-field corrections are taken into account. Our results are compared with the known van der Waals force between two ground-state atoms. To continuously interpolate between the two extreme cases of a single atom and a macroscopic sphere, we also derive the force between an atom and a sphere of variable radius that is embedded in an Onsager local-field cavity. Numerical examples illustrate the theory.

DOI: 10.1103/PhysRevA.81.012509 PACS number(s): 31.30.jh, 12.20.−m, 34.20.−b, 42.50.Wk

I. INTRODUCTION

Van der Waals (vdW) dispersion forces are effective electromagnetic forces that arise between polarizable objects as a consequence of correlated quantum fluctuations [1–10]. Postulated as early as 1873 to account for deviations from the ideal gas law [11], they were theoretically understood only much later in 1930, when London derived them from the electrostatic Coulomb interaction of charge fluctuations [12]. London found that two atoms of polarizabilities $\alpha_A(\omega)$ and $\alpha_B(\omega)$ at a distance r_{AB} are subject to a vdW potential

$$U(r_{AB}) = -\frac{3\hbar}{16\pi^3\varepsilon_0^2 r_{AB}^6}\int_0^\infty \mathrm{d}\xi\,\alpha_A(i\xi)\alpha_B(i\xi). \qquad (1)$$

Important progress was made in 1948 by Casimir and Polder, who included fluctuations of the transverse electromagnetic field and obtained a full quantum electrodynamic description of dispersion forces [13]. Their result reduces to the London formula in the electrostatic limit but is given by

$$U(r_{AB}) = -\frac{23\hbar c\alpha_A(0)\alpha_B(0)}{64\pi^3\varepsilon_0^2 r_{AB}^7} \qquad (2)$$

for distances much larger than the relevant atomic transition wavelengths.

Casimir arrived at his famous results while studying the properties of colloidal solutions [14]. These results illustrate the importance of dispersion forces to colloid science, which deals with the (inter alia vdW) interactions between small clusters of particles in free space [15] and, more often, with the different forces in colloidal suspensions. For example, (attractive) dispersion forces between spherical micro- and macro-objects embedded in a liquid [16] usually diminish the stability of such suspensions and may even cause clustering or flocculation [17]. The introduction of small amounts of highly charged nanoparticles gives rise to competing repulsive forces, thus balancing the stability of the suspension [18]. Stable mechanical suspensions might also be created with fluid-separated macro-objects such as eccentric cylinders by means of repulsive dispersion forces [19]. Note that in addition to dispersion and electrostatic forces, critical Casimir forces due to concentration fluctuations [20], chemical effects such as hydration and solvation, hydrophobic forces, and steric repulsion [21,22] and depletion [23] also influence the interaction of the colloidal particles.

Dispersion forces play a similar role in biology, where they contribute to the organization of molecules [24–26], cell adhesion [24,25,27,28], and the interaction of molecules with cell membranes [25,27]. They are also of interest in atomic force microscopy [29].

A large variety of models has been used in the past to study vdW forces between small polarizable objects [16]. Interacting atoms have been studied on a microscopic level as neutral arrangements of point charges [12,13], as sketched in Fig. 1(i). Larger systems can be treated by considering collections of such polarizable point objects [Fig. 1(ii)], in which a pairwise-sum method is often employed [30]. Investigations of the polarizability of N-atom nanoclusters of various sizes and shapes have shown that an additive relation, $\alpha_{\mathrm{clust}} = N\alpha_A$, does not hold in general but is valid for spherical clusters [31]. Microscopic approaches have to be contrasted with macroscopic descriptions in which continuous objects of polarizable matter are characterized by their permittivity [Fig. 1(iii)], and an intervening medium can be accounted for in the same spirit. One commonly distinguishes the additive Hamaker method [32] from the more elaborate Lifshitz theory, which includes many-body interactions [33,34].

A hybrid approach consists of a microscopic treatment of interacting atoms, combined with a macroscopic description of an intervening medium. To reconcile the microscopic and macroscopic pictures, local-field effects are included by assuming the atoms to be surrounded by small free-space cavities, an approach known as the Onsager real-cavity model [35]; see Fig. 1(iv). As found by studying the behavior of the classical Green tensor $\mathbf{G}$ for

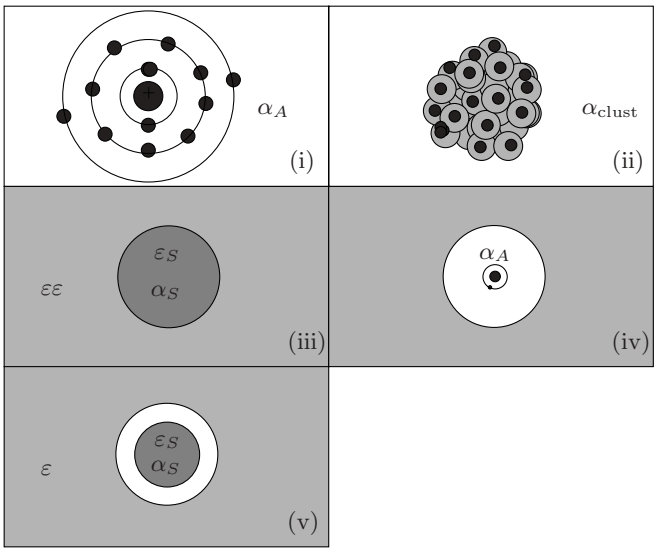

FIG. 1. Models of polarizable systems: (i) neutral arrangement of point charges (atom), (ii) cluster of atoms, (iii) dielectric sphere inside medium, (iv) atom in empty cavity surrounded by medium (Onsager real-cavity model), and (v) dielectric sphere in empty cavity surrounded by medium.

the electromagnetic field in conjunction with the real-cavity model [36], the vdW potential of two atoms at positions $\mathbf{r}_A$ and $\mathbf{r}_B$ in an arbitrary environment can be given as [37]

$$U(\mathbf{r}_A,\mathbf{r}_B) = -\frac{\hbar\mu_0^2}{2\pi}\int_0^\infty \mathrm{d}\xi\ \xi^4\alpha_A(i\xi)\alpha_B(i\xi) \times\left[\frac{3\varepsilon_A(i\xi)}{2\varepsilon_A(i\xi)+1}\right]^2\left[\frac{3\varepsilon_B(i\xi)}{2\varepsilon_B(i\xi)+1}\right]^2 \times \mathrm{Tr}[\mathbf{G}(\mathbf{r}_A,\mathbf{r}_B,i\xi)\cdot\mathbf{G}(\mathbf{r}_B,\mathbf{r}_A,i\xi)], \quad (3)$$

where local-field correction factors explicitly appear.

To compare the microscopic, local-field corrected approach of Fig. 1(iv) with the macroscopic one shown in Fig. 1(iii), in this work we study the Casimir-Polder (CP) interaction of a ground-state atom with a magnetodielectric sphere of variable size in the presence of arbitrary magnetoelectric background media on basis of macroscopic quantum electrodynamics (QED). Our considerations are related to free-space results obtained earlier for the interaction of an atom with curved surfaces [38] and dielectric [39] and perfectly conducting spheres [40]; compare with the nonretarded vdW potential of a ground-state atom inside and outside a dielectric or metallic spherical shell as calculated in Ref. [41]. In addition, we consider the interaction of an atom with a magnetodielectric sphere inside an Onsager cavity [Fig. 1(v)]. By changing the radius of the sphere, this construction allows us to study the transition between a microscopic pointlike object and a macroscopic one.

The article is organized as follows. In Sec. II, we recall the basic equations concerning ground-state CP potentials. In Sec. II A, we show how the Green tensors of a magnetodielectric full sphere or a sphere within an Onsager cavity can be written as functions of the Green tensors of the environment without the sphere. The results are then used to study the atom-sphere potentials, which are compared with the vdW interaction between two ground-state atoms (Sec. II B). As an example, we evaluate the interaction between an atom and molecules of different sizes in a bulk medium. A summary is given in Sec. III.

II. ATOM-SPHERE INTERACTION

In order to derive an expression for the CP interaction between a (ground-state) atom and a magnetodielectric sphere in the presence of an arbitrary medium environment, we start from the familiar formulas for the electric (U_e) and magnetic (U_m) CP potentials of a ground-state atom of polarizability

$$\alpha_A(\omega) = \lim_{\epsilon\to 0}\frac{2}{3\hbar}\sum_k \frac{\omega_{k0}|\mathbf{d}_{0k}|^2}{\omega_{k0}^2-\omega^2-i\omega\epsilon} \quad (4)$$

(where ω_{k0} are transition frequencies and $\mathbf{d}_{0k}$ are electric dipole matrix elements) and magnetizability

$$\beta_A(\omega) = \lim_{\epsilon\to 0}\frac{2}{3\hbar}\sum_k \frac{\omega_{k0}|\mathbf{m}_{0k}|^2}{\omega_{k0}^2-\omega^2-i\omega\epsilon} \quad (5)$$

(where $\mathbf{m}_{0k}$ are magnetic dipole matrix elements) that are placed at an arbitrary position $\mathbf{r}_A$ within an environment of locally and linearly responding magnetoelectric bodies or media [characterized by their permittivity $\varepsilon(\mathbf{r}_A,\omega)$ and permeability $\mu(\mathbf{r}_A,\omega)$] [7,37,42]:

$$U_e(\mathbf{r}_A) = \frac{\hbar\mu_0}{2\pi}\int_0^\infty \mathrm{d}\xi\ \xi^2\alpha_A(i\xi)\left[\frac{3\varepsilon_A(i\xi)}{2\varepsilon_A(i\xi)+1}\right]^2 \times \mathrm{Tr}\mathbf{G}^{(1)}(\mathbf{r}_A,\mathbf{r}_A,i\xi) \quad (6)$$

and

$$U_m(\mathbf{r}_A) = \frac{\hbar\mu_0}{2\pi}\int_0^\infty \mathrm{d}\xi\beta_A(i\xi)\left[\frac{3}{2\mu_A(i\xi)+1}\right]^2 \times \mathrm{Tr}[\nabla\times\mathbf{G}^{(1)}(\mathbf{r}_A,\mathbf{r}_A,i\xi)\times\overleftarrow{\nabla}'], \quad (7)$$

with $\varepsilon_A(\omega)\equiv\varepsilon(\mathbf{r}_A,\omega)$, $\mu_A(\omega)\equiv\mu(\mathbf{r}_A,\omega)$. These expressions explicitly allow for the atom to be embedded in a medium environment where the relevant local-field corrections have been accounted for via the Onsager real-cavity model [35,36]. The scattering Green tensor $\mathbf{G}^{(1)}(\mathbf{r},\mathbf{r}',\omega)$ fully accounts for the position, size, and shape of all bodies and media as well as their magnetoelectric properties and is defined by the differential equation

$$\left[\nabla\times\frac{1}{\mu(\mathbf{r},\omega)}\nabla\times-\frac{\omega^2}{c^2}\varepsilon(\mathbf{r},\omega)\right]\mathbf{G}(\mathbf{r},\mathbf{r}',\omega) = \boldsymbol{\delta}(\mathbf{r}-\mathbf{r}'), \quad (8)$$

with the condition $\mathbf{G}(\mathbf{r},\mathbf{r}',\omega)\to\mathbf{0}$ for $|\mathbf{r}-\mathbf{r}'|\to\infty$. In this work, the body interacting with the atom is a magnetodielectric sphere whose Green tensor we analyze in the following.

A. Decomposition of the Green tensor

Two methods may be envisaged to study the CP potential of an atom in the presence of a magnetodielectric sphere and an arbitrary environment of additional bodies and media. First, one could work with the Green tensor of the combined sphere-environment system [Fig. 2(i)] directly, which may be very

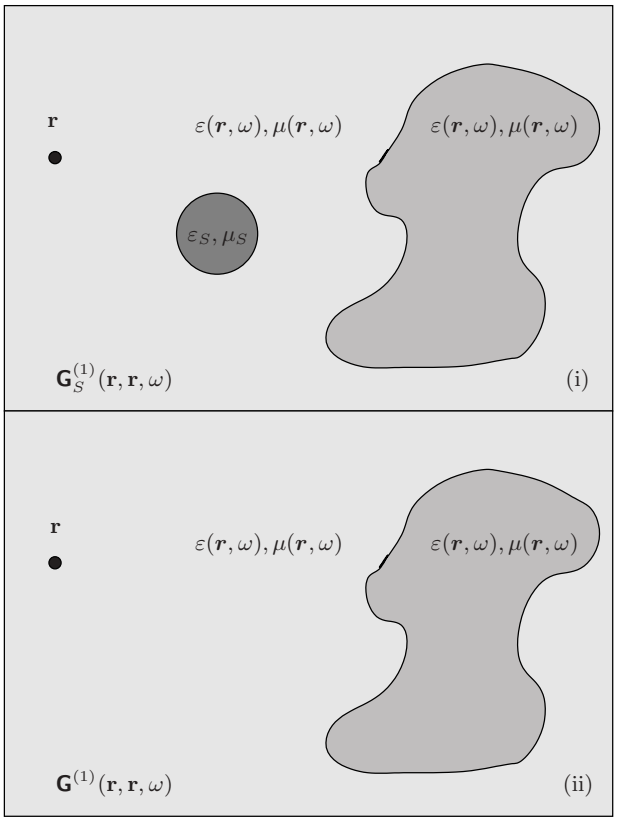

FIG. 2. (i) Green tensor of the combined system of magnetodielectric sphere and arbitrary background environment and (ii) Green tensor of the same system without the sphere.

complicated; even if an analytical expression of the Green tensor is known, the resulting expressions for the potentials are hard to evaluate and do not allow for an explicit discussion of the influence of the sphere. In this work, we therefore follow a second, alternative approach: We show how the Green tensor of the full arrangement including the sphere, $\mathbf{G}_S^{(1)}(\mathbf{r},\mathbf{r},\omega)$, can be related to the Green tensor without the sphere [Fig. 2(ii)]; $\mathbf{G}^{(1)}(\mathbf{r},\mathbf{r},\omega)$ describes only the background environment. To establish such a relation, we use methods similar to those developed for studying local-field corrections [36,37,42]. The crucial assumption for using these point-scattering techniques is that the effective radius of the sphere is small compared with the relevant wavelengths of the electromagnetic field.

1. Full sphere

Assuming that the functions $\varepsilon(\mathbf{r},\omega)$ and $\mu(\mathbf{r},\omega)$ describe the magnetoelectric properties of the environment, the introduction of a homogeneous magnetodielectric sphere with radius R centered at $\mathbf{r}_S$, permittivity $\varepsilon_S(\omega)$, and permeability $\mu_S(\omega)$ leads to the new functions

$$\varepsilon_S(\mathbf{r},\omega),\ \mu_S(\mathbf{r},\omega) = \begin{cases} \varepsilon_S(\omega),\ \mu_S(\omega) & \text{for } |\mathbf{r}-\mathbf{r}_S| \leqslant R, \\ \varepsilon(\mathbf{r},\omega),\ \mu(\mathbf{r},\omega) & \text{elsewhere.} \end{cases} \tag{9}$$

The Green tensor $\mathbf{G}_S^{(1)}(\mathbf{r},\mathbf{r},\omega)$ of sphere plus environment is hence the solution to the differential equation (8) with $\varepsilon_S(\mathbf{r},\omega)$ and $\mu_S(\mathbf{r},\omega)$ in place of $\varepsilon(\mathbf{r},\omega)$ and $\mu(\mathbf{r},\omega)$.

As discussed in Refs. [36,37], for a small sphere it is sufficient to consider first the special case of a homogeneous, bulk environment, which is then generalized to arbitrary environments at the end of the section. The required scattering Green tensor of the sphere with center $\mathbf{r}_S = \mathbf{0}$ inside a bulk medium of permittivity $\varepsilon(\omega)$ and permeability $\mu(\omega)$ can be written in the form [43]

$$\begin{aligned} \mathbf{G}_S^{(1)}(\mathbf{r},\mathbf{r}',\omega) = {} & \frac{i\mu k}{4\pi}\sum_{p=\pm}\sum_{l=1}^{\infty}\sum_{m=0}^{n}(2-\delta_{m0}) \\ & \times \frac{2l+1}{l(l+1)}\frac{(l-m)!}{(l+m)!} \\ & \times \left[B_l^M \mathbf{M}_{lmp}(k,\mathbf{r})\mathbf{M}_{lmp}(k,\mathbf{r}') \right. \\ & \left. + B_l^N \mathbf{N}_{lmp}(k,\mathbf{r})\mathbf{N}_{lmp}(k,\mathbf{r}')\right], \end{aligned} \tag{10}$$

where $k = \sqrt{\varepsilon\mu}\omega/c$, $\mathbf{M}_{lmp}$, $\mathbf{N}_{lmp}$ denote even (+) and odd (−) spherical vector wave functions with total angular momentum l and z projection m, and $B_l^{M,N}$ are the associated coefficients for reflection at the surface of the sphere. Explicit forms for $\mathbf{M}_{lmp}$, $\mathbf{N}_{lmp}$, and $B_l^{M,N}$ can be found in Refs. [43,44].

In the limit of a small sphere with $|k_S R|, |kR| \ll 1$ ($k_S = \sqrt{\varepsilon_S\mu_S}\omega/c$), we have

$$B_l^{M,N} = O\left(\frac{\omega R}{c}\right)^{2l+1}, \tag{11}$$

and so the dominant contribution to the Green tensor is due to the $l = 1$ terms. The respective vector wave functions are given by

$$\begin{aligned} \mathbf{M}_{1m\pm}(k,\mathbf{r}) = {} & \mp\frac{m}{\sin\theta}h_1^{(1)}(kr)P_1^m(\cos\theta)\begin{Bmatrix}\sin m\phi\\ \cos m\phi\end{Bmatrix}\mathbf{e}_\theta \\ & - h_1^{(1)}(kr)\frac{\mathrm{d}P_1^m(\cos\theta)}{\mathrm{d}\theta}\begin{Bmatrix}\cos m\phi\\ \sin m\phi\end{Bmatrix}\mathbf{e}_\phi \end{aligned} \tag{12}$$

and

$$\begin{aligned} \mathbf{N}_{1m\pm}(\mathbf{r}) = {} & 2\frac{h_1^{(1)}(kr)}{kr}P_1^m(\cos\theta)\begin{Bmatrix}\cos m\phi\\ \sin m\phi\end{Bmatrix}\mathbf{e}_r \\ & + \frac{1}{kr}\frac{\mathrm{d}\left[krh_1^{(1)}(kr)\right]}{d(kr)}\frac{\mathrm{d}P_1^m(\cos\theta)}{\mathrm{d}\theta}\begin{Bmatrix}\cos m\phi\\ \sin m\phi\end{Bmatrix}\mathbf{e}_\theta \\ & \mp\frac{m}{\sin\theta}P_1^m(\cos\theta)\frac{1}{kr}\frac{\mathrm{d}\left[krh_1^{(1)}(kr)\right]}{d(kr)}\begin{Bmatrix}\sin m\phi\\ \cos m\phi\end{Bmatrix}\mathbf{e}_\phi, \end{aligned} \tag{13}$$

where the $P_1^m(x)$ are associated Legendre polynomials and $h_1^{(1)}(x)$ is a spherical Hankel function of the first kind. The $l = 1$ reflection coefficients in the small-sphere limit $|k_S R|, |kR| \ll 1$ are given by

$$B_1^M = \frac{2i}{3}\left(\sqrt{\varepsilon\mu}\frac{\omega R}{c}\right)^3\frac{\mu_S-\mu}{\mu_S+2\mu}, \tag{14}$$

$$B_1^N = \frac{2i}{3}\left(\sqrt{\varepsilon\mu}\frac{\omega R}{c}\right)^3\frac{\varepsilon_S-\varepsilon}{\varepsilon_S+2\varepsilon}. \tag{15}$$

We can further evaluate the p and m sums for $l=1$ using $P_1^0(\cos\theta)=\cos\theta$ and $P_1^1(\cos\theta)=-\sin\theta$ to obtain

$$\sum_{p=\pm1}\sum_{m=0}^{1}(2-\delta_{m0})\frac{(1-m)!}{(1+m)!}\mathbf{M}_{1mp}(\mathbf{r})\mathbf{M}_{1mp}(\mathbf{r})=h^2[\mathbf{l}-\mathbf{e}_r\mathbf{e}_r] \tag{16}$$

and

$$\sum_{p=\pm1}\sum_{m=0}^{1}(2-\delta_{m0})\frac{(1-m)!}{(1+m)!}\mathbf{N}_{1mp}(\mathbf{r})\mathbf{N}_{1mp}(\mathbf{r}) = \frac{h'^2}{(kr)^2}\mathbf{l}+\frac{4h^2-h'^2}{(kr)^2}\mathbf{e}_r\mathbf{e}_r, \tag{17}$$

with the notation $h\equiv h_1^{(1)}(kr)=-i(1-ikr)e^{ikr}/(kr)^2$ and $h'\equiv \mathrm{d}[krh_1^{(1)}(kr)]/\mathrm{d}(kr)$. By substituting these expressions into Eq. (10), the (equal-position) scattering Green tensor of a small sphere becomes

$$\begin{aligned}\mathbf{G}_S^{(1)}(\mathbf{r},\mathbf{r},\omega)=\frac{\mu e^{2ikr}}{4\pi k^2r^6}&\{[1-2ikr-3(kr)^2+2i(kr)^3+(kr)^4]\mathbf{l}\\&+[3-6ikr-(kr)^2-2i(kr)^3-(kr)^4]\mathbf{e}_r\mathbf{e}_r\}\\&\times\frac{\varepsilon_S-\varepsilon}{\varepsilon_S+2\varepsilon}R^3+\frac{\mu e^{2ikr}}{4\pi r^4}[1-2ikr-(kr)^2]\\&\times(\mathbf{l}-\mathbf{e}_r\mathbf{e}_r)\frac{\mu_S-\mu}{\mu_S+2\mu}R^3.\end{aligned} \tag{18}$$

Next, we relate our result to the Green tensor of the bulk medium without the sphere (cf., e.g., Ref. [44]),

$$\begin{aligned}\mathbf{G}(\mathbf{r},\mathbf{r}',\omega)=-\frac{\mu e^{ik\rho}}{4\pi k^2\rho^3}&\{[1-ik\rho-(k\rho)^2)]\mathbf{l}\\&-[3-3ik\rho-(k\rho)^2]\mathbf{e}_\rho\mathbf{e}_\rho\},\end{aligned} \tag{19}$$

which is valid for $\mathbf{r}\neq\mathbf{r}'$, where $\boldsymbol{\rho}=\mathbf{r}-\mathbf{r}'$, $\rho=|\boldsymbol{\rho}|$, and $\mathbf{e}_\rho=\boldsymbol{\rho}/\rho$. The Green tensor $\mathbf{G}_S^{(1)}(\mathbf{r},\mathbf{r},\omega)$ of the small sphere describes the propagation of the electric field from a source at $\mathbf{r}$ to the sphere, its scattering from the sphere (a polarizable and magnetizable point scatterer) at $\mathbf{r}_S=\mathbf{0}$, and its return to $\mathbf{r}$. It is therefore natural to try and compose $\mathbf{G}_S^{(1)}$ from products of $\mathbf{G}$, which describes the propagation of the electric field through the bulk medium to an electric scatterer, and $\mathbf{G}\times\overleftarrow{\nabla}$, which describes its propagation to a magnetic scatterer. Indeed, from Eq. (19), we find that

$$\begin{aligned}&\mathbf{G}(\mathbf{r},\mathbf{0},\omega)\cdot\mathbf{G}(\mathbf{0},\mathbf{r},\omega)\\&=\frac{\mu^2e^{2ikr}}{16\pi^2k^4r^6}\{[1-2ikr-3(kr)^2+2i(kr)^3+(kr)^4]\mathbf{l}\\&\quad+[3-6ikr-(kr)^2-2i(kr)^3-(kr)^4]\,\mathbf{e}_r\mathbf{e}_r\}\end{aligned} \tag{20}$$

and

$$\begin{aligned}&\mathbf{G}(\mathbf{r},\mathbf{r}_S,\omega)\times\overleftarrow{\nabla}_S\cdot\nabla_S\times\mathbf{G}(\mathbf{r}_S,\mathbf{r},\omega)|_{\mathbf{r}_S=\mathbf{0}}\\&=-\frac{\mu^2e^{2ikr}}{16\pi^2r^4}[1-2ikr-(kr)^2](\mathbf{l}-\mathbf{e}_r\mathbf{e}_r).\end{aligned} \tag{21}$$

A comparison with Eq. (18) shows that

$$\begin{aligned}\mathbf{G}_S^{(1)}(\mathbf{r},\mathbf{r},\omega)=4\pi\varepsilon R^3\frac{\varepsilon_S-\varepsilon}{\varepsilon_S+2\varepsilon}\frac{\omega^2}{c^2}&\mathbf{G}(\mathbf{r},\mathbf{0},\omega)\cdot\mathbf{G}(\mathbf{0},\mathbf{r},\omega)\\&-\frac{4\pi R^3}{\mu}\frac{\mu_S-\mu}{\mu_S+2\mu}\mathbf{G}(\mathbf{r},\mathbf{r}_S,\omega)\times\overleftarrow{\nabla}_S\\&\cdot\nabla_S\times\mathbf{G}(\mathbf{r}_S,\mathbf{r},\omega)|_{\mathbf{r}_S=\mathbf{0}}.\end{aligned} \tag{22}$$

Let us next consider a general background environment, which can involve different media or bodies, as sketched in Fig. 2. With the permittivity $\varepsilon(\mathbf{r},\omega)$ and permeability $\mu(\mathbf{r},\omega)$ of the environment now being functions of position, it is useful to introduce a notation for their values at the position of the sphere, $\varepsilon_\odot(\omega)\equiv\varepsilon(\mathbf{r}_S,\omega)$, $\mu_\odot(\omega)\equiv\mu(\mathbf{r}_S,\omega)$. In addition to the small-sphere limit $|k_SR|\ll1$, we assume the effective sphere radius $\sqrt{\varepsilon_S\mu_S}R$ to be much smaller than the distance from the sphere to any of the environment bodies. As demonstrated in Refs. [36,37], multiple scattering between sphere and environment can then be safely neglected to within a leading order of k_SR, and a result of the type (22) can be generalized from the bulk case to an arbitrary environment by adding the scattering Green tensor and replacing $\varepsilon\mapsto\varepsilon_\odot$ and $\mu\mapsto\mu_\odot$. This can be formally proven by treating both the sphere and the environment bodies using a Born expansion of the Green tensor [45] and discarding those terms in the Born series that involve multiple scattering between atom and environment. We obtain

$$\begin{aligned}\mathbf{G}_S^{(1)}(\mathbf{r},\mathbf{r},\omega)=\mathbf{G}^{(1)}(\mathbf{r},\mathbf{r},\omega)+\frac{\varepsilon_\odot}{\varepsilon_0}\alpha_S^\star\frac{\omega^2}{c^2}&\mathbf{G}(\mathbf{r},\mathbf{r}_S,\omega)\\&\cdot\mathbf{G}(\mathbf{r}_S,\mathbf{r},\omega)-\frac{\mu_0}{\mu_\odot}\beta_S^\star\mathbf{G}(\mathbf{r},\mathbf{r}_S,\omega)\times\overleftarrow{\nabla}_S\\&\cdot\nabla_S\times\mathbf{G}(\mathbf{r}_S,\mathbf{r},\omega),\end{aligned} \tag{23}$$

where we have introduced the polarizability

$$\alpha_S^\star=4\pi\varepsilon_0R^3\frac{\varepsilon_S-\varepsilon_\odot}{\varepsilon_S+2\varepsilon_\odot} \tag{24}$$

and the magnetizability

$$\beta_S^\star=\frac{4\pi R^3}{\mu_0}\frac{\mu_S-\mu_\odot}{\mu_S+2\mu_\odot} \tag{25}$$

of the sphere [46]. Note that $\alpha_S^\star$ is an excess or effective polarizability [47,48] and describes the electric response of the sphere with respect to that of the surrounding medium. It can take positive or negative values, depending on whether the sphere's permittivity is larger or smaller than that of the medium.

The relation (23) for $\mathbf{G}_S^{(1)}$ can be used to calculate the electric CP potential (6). In order to find the magnetic CP potential, Eq. (7), we also require the analogous relation for the magnetic Green tensor $\nabla\times\mathbf{G}_S^{(1)}\times\overleftarrow{\nabla}'$, which can be obtained by duality arguments. An electric/magnetic duality transformation $[\cdot]^\circledast$ corresponds to a global exchange of electric and magnetic properties, $\varepsilon^\circledast=\mu$ and $\mu^\circledast=\varepsilon$. As shown in Refs. [49,50], this results in the following changes to the Green tensor

for $\mathbf{r} \neq \mathbf{r}'$:

$$\frac{\omega^2}{c^2}\mathbf{G}^{\circledast}(\mathbf{r},\mathbf{r}',\omega) = -\frac{\nabla\times\mathbf{G}(\mathbf{r},\mathbf{r}',\omega)\times\overleftarrow{\nabla}'}{\mu(\mathbf{r},\omega)\mu(\mathbf{r}',\omega)}, \tag{26}$$

$$\nabla\times\mathbf{G}^{\circledast}(\mathbf{r},\mathbf{r}',\omega)\times\overleftarrow{\nabla}' = -\varepsilon(\mathbf{r},\omega)\frac{\omega^2}{c^2}\mathbf{G}(\mathbf{r},\mathbf{r}',\omega)\varepsilon(\mathbf{r}',\omega), \tag{27}$$

$$\nabla\times\mathbf{G}^{\circledast}(\mathbf{r},\mathbf{r}',\omega) = -\varepsilon(\mathbf{r},\omega)\frac{\mathbf{G}(\mathbf{r},\mathbf{r}',\omega)\times\overleftarrow{\nabla}'}{\mu(\mathbf{r}',\omega)}, \tag{28}$$

$$\mathbf{G}^{\circledast}(\mathbf{r},\mathbf{r}',\omega)\times\overleftarrow{\nabla}' = -\frac{\nabla\times\mathbf{G}(\mathbf{r},\mathbf{r}',\omega)}{\mu(\mathbf{r},\omega)}\varepsilon(\mathbf{r}',\omega). \tag{29}$$

In addition, Eqs. (24) and (25) imply that $\alpha_S^{\star\circledast} = \beta_S^{\star}/c^2$ and $\beta_S^{\star\circledast} = c^2\alpha_S^{\star}$. By applying the duality transformation to both sides of Eq. (23), one obtains the required relation

$$\begin{aligned}\nabla\times\mathbf{G}_S^{(1)}(\mathbf{r},\mathbf{r}',\omega)\times\overleftarrow{\nabla}'|_{\mathbf{r}'=\mathbf{r}}&\\ = \nabla\times\mathbf{G}^{(1)}(\mathbf{r},\mathbf{r}',\omega)\times\overleftarrow{\nabla}'|_{\mathbf{r}'=\mathbf{r}} - \frac{\mu_0}{\mu_\odot}\beta_S^{\star}\nabla\times\mathbf{G}(\mathbf{r},\mathbf{r}_S,\omega)\times\overleftarrow{\nabla}_S&\\ \cdot\nabla_S\times\mathbf{G}(\mathbf{r}_S,\mathbf{r}',\omega)\times\overleftarrow{\nabla}'|_{\mathbf{r}'=\mathbf{r}} + \frac{\varepsilon_\odot}{\varepsilon_0}\alpha_S^{\star}\frac{\omega^2}{c^2}&\\ \times\nabla\times\mathbf{G}(\mathbf{r},\mathbf{r}_S,\omega)\cdot\mathbf{G}(\mathbf{r}_S,\mathbf{r}',\omega)\times\overleftarrow{\nabla}'|_{\mathbf{r}'=\mathbf{r}}.&\end{aligned} \tag{30}$$

2. *Sphere inside an Onsager cavity*

Next, we consider a homogeneous magnetodielectric sphere with radius R centered around $\mathbf{r}_S$, with permittivity $\varepsilon_S(\omega)$ and permeability $\mu_S(\omega)$, which is not in immediate contact with the surrounding medium but is placed inside a small spherical cavity of radius R_C, also centered around $\mathbf{r}_S$ [Fig. 1(v)]. This enables us to compare and interpolate between the homogeneous sphere placed inside a medium (as considered in the previous section) and a local-field-corrected atom (i.e., a pointlike polarizable system surrounded by a cavity). The scattering Green tensor $\mathbf{G}_{S+C}^{(1)}$ of the sphere-plus-cavity system in a homogeneous bulk medium is again given by an equation of the form (10), in which the reflection coefficients take a more complex form. In particular, in the limit of a small effective cavity and sphere sizes $|k_S R|, |kR_C| \ll 1$, one has [44]

$$B_1^M = \frac{2i}{3}\left(\sqrt{\varepsilon\mu}\frac{\omega}{c}\right)^3\left[R_C^3\frac{1-\mu}{1+2\mu} + \frac{9\mu R^3(\mu_S-1)/(2\mu+1)}{(\mu_S+2)(2\mu+1)+2(\mu_S-1)(1-\mu)R^3/R_C^3}\right], \tag{31}$$

$$B_1^N = \frac{2i}{3}\left(\sqrt{\varepsilon\mu}\frac{\omega}{c}\right)^3\left[R_C^3\frac{1-\varepsilon}{1+2\varepsilon} + \frac{9\varepsilon R^3(\varepsilon_S-1)/(2\varepsilon+1)}{(\varepsilon_S+2)(2\varepsilon+1)+2(\varepsilon_S-1)(1-\varepsilon)R^3/R_C^3}\right]. \tag{32}$$

We can then follow exactly the same steps as in Sec. II A 1. We again arrive at Eqs. (23) and (30) with $S+C$ in place of S. A comparison of Eqs. (14) and (15) with Eqs. (31) and (32) shows that the relevant excess polarizability and magnetizability of the sphere-plus-cavity system are given by

$$\alpha_{S+C}^{\star} = 4\pi\varepsilon_0\left[R_C^3\frac{1-\varepsilon_\odot}{1+2\varepsilon_\odot} + \frac{9\varepsilon_\odot R^3(\varepsilon_S-1)/(2\varepsilon_\odot+1)}{(\varepsilon_S+2)(2\varepsilon_\odot+1)+2(\varepsilon_S-1)(1-\varepsilon_\odot)R^3/R_C^3}\right] \tag{33}$$

and

$$\beta_{S+C}^{\star} = \frac{4\pi}{\mu_0}\left[R_C^3\frac{1-\mu_\odot}{1+2\mu_\odot} + \frac{9\mu_\odot R^3(\mu_S-1)/(2\mu_\odot+1)}{(\mu_S+2)(2\mu_\odot+1)+2(\mu_S-1)(1-\mu_\odot)R^3/R_C^3}\right]. \tag{34}$$

One can easily verify that for $R = R_C$, Eqs. (33) and (34) reduce to the results (24) and (25) for the full sphere, as expected.

By introducing the free-space polarizability and magnetizability of the sphere,

$$\alpha_S = 4\pi\varepsilon_0 R^3\frac{\varepsilon_S-1}{\varepsilon_S+2} \tag{35}$$

and

$$\beta_S = \frac{4\pi R^3}{\mu_0}\frac{\mu_S-1}{\mu_S+2}, \tag{36}$$

as well as the excess polarizability and magnetizability of the cavity,

$$\alpha_C^{\star} = 4\pi\varepsilon_0 R_C^3\frac{1-\varepsilon_\odot}{1+2\varepsilon_\odot} \tag{37}$$

and

$$\beta_C^{\star} = \frac{4\pi R_C^3}{\mu_0}\frac{1-\mu_\odot}{1+2\mu_\odot}, \tag{38}$$

we can write Eqs. (33) and (34) more transparently as

$$\alpha_{S+C}^{\star} = \alpha_C^{\star} + \frac{\alpha_S}{\varepsilon_\odot}\left(\frac{3\varepsilon_\odot}{2\varepsilon_\odot+1}\right)^2 \times\frac{1}{1+\alpha_C^{\star}\alpha_S/\left(8\pi^2\varepsilon_0^2R_C^6\right)}, \tag{39}$$

$$\beta_{S+C}^{\star} = \beta_C^{\star} + \beta_S\mu_\odot\left(\frac{3}{2\mu_\odot+1}\right)^2 \times\frac{1}{1+\beta_C^{\star}\beta_S\mu_0^2/\left(8\pi^2R_C^6\right)}. \tag{40}$$

As we see, the response of the sphere-plus-cavity system to an electromagnetic field is due to reflection at the cavity surface from the outside ($\alpha_C^{\star}$,$\beta_C^{\star}$) plus reflections at the sphere ($\alpha_S^{\star}$,$\beta_S^{\star}$), in which the local-field correction factors in large round brackets account for the transmission of the field into and out of the cavity and the denominators account for multiple reflections between the cavity and sphere surfaces.

Note that in our leading-order approximation in terms of the cavity and sphere radii, the reflective properties of the cavity and the sphere as encoded via their dipole polarizabilities and magnetizabilities are proportional to the third

power of these radii. In contrast, the transmission properties of the cavity as described by the local-field correction factors become independent of R_C within leading order of kR_C.

B. Casimir-Polder potential

Consider a polarizable and magnetizable ground-state atom that interacts with a small magnetodielectric sphere in an arbitrary environment. We assume the atom-sphere separation r_{AS} to be much greater than the effective sphere and cavity radii, $\sqrt{\varepsilon_S\mu_S}R$, $\sqrt{\varepsilon_\odot\mu_\odot}R_C \ll r_{AS}$. For the frequency integral in Eq. (6), typically limited to values $\xi \leqslant c/r_{AS}$, the assumptions $|k_S R|, |kR_C| \ll 1$ made in Sec. II A hold. Hence, we can use our results for the electric and magnetic Green tensors $\mathbf{G}_S^{(1)}$ and $\nabla \times \mathbf{G}_S^{(1)} \times \overleftarrow{\nabla}'$ in the presence of a small magnetodielectric sphere to calculate the atom-sphere potential.

1. Full sphere

By substituting Eq. (23) into Eq. (6), the interaction of an electric atom with a magnetodielectric sphere is described by the potential

$$U_e(\mathbf{r}_A, \mathbf{r}_S) = U_{ee}(\mathbf{r}_A, \mathbf{r}_S) + U_{em}(\mathbf{r}_A, \mathbf{r}_S), \tag{41}$$

with

$$U_{ee}(\mathbf{r}_A, \mathbf{r}_S) = -\frac{\hbar\mu_0^2}{2\pi}\int_0^\infty \mathrm{d}\xi\ \xi^4\alpha_A(i\xi)\left[\frac{3\varepsilon_A(i\xi)}{2\varepsilon_A(i\xi)+1}\right]^2 \times \alpha_S(i\xi)\varepsilon_\odot(i\xi)\mathrm{Tr}[\mathbf{G}(\mathbf{r}_A, \mathbf{r}_S, i\xi)\cdot\mathbf{G}(\mathbf{r}_S, \mathbf{r}_A, i\xi)] \tag{42}$$

and

$$U_{em}(\mathbf{r}_A, \mathbf{r}_S) = -\frac{\hbar\mu_0^2}{2\pi}\int_0^\infty \mathrm{d}\xi\ \xi^2\alpha_A(i\xi)\left[\frac{3\varepsilon_A(i\xi)}{2\varepsilon_A(i\xi)+1}\right]^2 \times \frac{\beta_S(i\xi)}{\mu_\odot(i\xi)}\mathrm{Tr}[\mathbf{G}(\mathbf{r}_A, \mathbf{r}_S, i\xi)\times\overleftarrow{\nabla}_S\cdot\nabla_S \times \mathbf{G}(\mathbf{r}_S, \mathbf{r}_A, i\xi)] \tag{43}$$

being associated with the electric and magnetic properties of the sphere, respectively. Similarly, combining Eqs. (30) and (7) gives the CP interaction of a magnetic atom and a magnetodielectric sphere,

$$U_m(\mathbf{r}_A, \mathbf{r}_S) = U_{me}(\mathbf{r}_A, \mathbf{r}_S) + U_{mm}(\mathbf{r}_A, \mathbf{r}_S), \tag{44}$$

with

$$U_{me}(\mathbf{r}_A, \mathbf{r}_S) = -\frac{\hbar\mu_0^2}{2\pi}\int_0^\infty \mathrm{d}\xi\ \xi^2\beta_A(i\xi)\left[\frac{3}{2\mu_A(i\xi)+1}\right]^2 \times \alpha_S(i\xi)\varepsilon_\odot(i\xi)\mathrm{Tr}\{[\nabla_A \times \mathbf{G}(\mathbf{r}_A, \mathbf{r}_S, i\xi)] \cdot [\mathbf{G}(\mathbf{r}_S, \mathbf{r}_A, i\xi)\times\overleftarrow{\nabla}_A]\} \tag{45}$$

and

$$U_{mm}(\mathbf{r}_A, \mathbf{r}_S) = -\frac{\hbar\mu_0^2}{2\pi}\int_0^\infty \mathrm{d}\xi\beta_A(i\xi)\left[\frac{3}{2\mu_A(i\xi)+1}\right]^2 \times \frac{\beta_S(i\xi)}{\mu_\odot(i\xi)}\mathrm{Tr}\{[\nabla_A \times \mathbf{G}(\mathbf{r}_A, \mathbf{r}_S, i\xi)\times\overleftarrow{\nabla}_S] \cdot [\nabla_S \times \mathbf{G}(\mathbf{r}_S, \mathbf{r}_A, i\xi)\times\overleftarrow{\nabla}_A]\}. \tag{46}$$

Note that the electric and magnetic properties of the sphere completely decouple and give rise to the separate potentials U_{ee}, U_{me} and U_{em}, U_{mm}, respectively. However, this is only true in the small-sphere limit considered here.

As proven in Refs. [49,50], the local-field-corrected total CP potential of a magnetodielectric ground-state atom in the presence of an arbitrary arrangement of bodies as given by Eqs. (6) and (7) is always duality invariant. By using the transformation rules (26)–(29) for the Green tensor, together with $\alpha^{\star\circledast} = \beta^\star/c^2$, $\beta^{\star\circledast} = c^2\alpha^\star$, one sees that duality invariance also holds for the special case of a sphere, where $U_{ee}(\mathbf{r}_A, \mathbf{r}_S)^\circledast = U_{mm}(\mathbf{r}_A, \mathbf{r}_S)$ and $U_{em}(\mathbf{r}_A, \mathbf{r}_S)^\circledast = U_{me}(\mathbf{r}_A, \mathbf{r}_S)$. This property is ensured by the presence of the factors $\varepsilon_\odot$ and $1/\mu_\odot$ in Eqs. (42), (43), (45), and (46).

It is instructive to compare our findings with the vdW interaction between two magnetodielectric ground-state atoms A and B in the presence of an arbitrary magnetodielectric environment [37,42]. In order to reproduce those results, one has to perform the substitutions

$$\alpha_S\varepsilon_\odot \to \alpha_B\left(\frac{3\varepsilon_B}{2\varepsilon_B+1}\right)^2 \tag{47}$$

and

$$\frac{\beta_S}{\mu_\odot} \to \beta_B\left(\frac{3}{2\mu_B+1}\right)^2. \tag{48}$$

The differences between the cases of a sphere [left-hand sides of Eqs. (47) and (48)] and an atom [right-hand sides] are due to the microscopic and macroscopic nature of the two objects. The sphere consists of a large number of atoms whose magnetoelectric response can be described by an average permittivity and permeability. In this macroscopic picture, the sphere is in immediate contact with the surrounding medium (also characterized by permittivity and permeability), which leads to the factors $\varepsilon_\odot$ and $1/\mu_\odot$. In contrast, an atom is a microscopic object. In the microscopic picture, the interspace between the atom and the neighboring medium atoms needs to be taken into account; it gives rise to the local-field correction factors on the right-hand sides of Eqs. (47) and (48).

The second difference between the two cases is in the different explicit forms of polarizability and magnetizability. For a sphere, they are given in terms of the permeability and permittivity of the sphere in comparison to those of the surrounding medium [cf. Eqs. (24) and (25)]; they can be either positive or negative. For an atom, polarizability and magnetizability depend on the transition frequencies and dipole matrix elements [recall Eqs. (4) and (5)]; they are strictly positive on the positive imaginary frequency axis.

2. Sphere inside an Onsager cavity

In order to interpolate between the two extreme cases of a single atom and a sphere consisting of a very large number of atoms, we now consider the CP interaction of an atom with a sphere of radius R that is separated from the surrounding medium by a spherical free-space cavity of radius R_C, as introduced in Sec. II A 2. Since expressions of the type (23) and (30) remain valid, their substitution into Eqs. (6) and (7) again leads to Eqs. (41)–(46), where now $\alpha_{S+C}^\star$ and $\beta_{S+C}^\star$ as given by Eqs. (33) and (34) appear in place of $\alpha_S^\star$ and $\beta_S^\star$.

In our model, the sphere may consist of an arbitrary number of atoms, whereas the cavity implements the interspace between the sphere's atoms and the surrounding medium atoms. As seen from Eqs. (39) and (40) for the polarizability and magnetizability of the sphere-plus-cavity system, the sphere is represented by its free-space polarizability and magnetizability, whereas the interspace gives rise to the cavity excess polarizability and magnetizability. In the purely electric case, the sphere gives rise to attractive forces and the cavity leads to a reduction of these forces.

For a sphere that consists of a very large number of atoms, the interspace between the sphere and medium atoms becomes irrelevant. In this case, which is implemented by the limit $R \to R_C$, the system's polarizability and magnetizability become equal to the excess polarizability and magnetizability of a full sphere (recall Sec. II A2), for which we recover Eqs. (41)–(46) in their original form.

In the opposite extreme case of a sphere that consists of very few atoms, the interspace becomes very large in comparison to the sphere, $R \ll R_C$. In this limit, the effect of multiple scattering between the surfaces of sphere and cavity becomes negligible, and the polarizability (39) and magnetizability (40) reduce to

$$\alpha^{\star}_{S+C} = \alpha^{\star}_{C} + \frac{\alpha_S}{\varepsilon_\odot}\left(\frac{3\varepsilon_\odot}{2\varepsilon_\odot+1}\right)^2 \tag{49}$$

and

$$\beta^{\star}_{S+C} = \beta^{\star}_{C} + \beta_S\mu_\odot\left(\frac{3}{2\mu_\odot+1}\right)^2. \tag{50}$$

When the sphere consists of only a single atom B, the Clausius-Mossotti laws [51]

$$\frac{\varepsilon_S-1}{\varepsilon_S+2} = \frac{\alpha_B}{3\varepsilon_0 V}, \quad \frac{\mu_S-1}{\mu_S+2} = \frac{\mu_0\beta_B}{3V}, \tag{51}$$

where $V = (4\pi/3)R^3$, together with Eqs. (35) and (36), show that $\alpha_S = \alpha_B$ and $\beta_S = \beta_B$. When neglecting the backscattering from the outside surface of the cavity, we obtain

$$\alpha_{S+C}\varepsilon_\odot = \alpha_B\left(\frac{3\varepsilon_B}{2\varepsilon_B+1}\right)^2 \tag{52}$$

and

$$\frac{\beta_{S+C}}{\mu_\odot} = \beta_B\left(\frac{3}{2\mu_B+1}\right)^2, \tag{53}$$

where $\varepsilon_\odot = \varepsilon_B, \mu_\odot = \mu_B$, and substitution into Eqs. (41)–(46) leads to the local-field-corrected two-atom potentials [37,42]. It is in this limit $R \ll R_C, \sqrt{\varepsilon_\odot\mu_\odot}R_C \ll r_{AS}$ that the potential depends on the cavity radius only via its transmission properties and therefore becomes independent of R_C. Recall the discussion following Eq. (40).

For intermediate radii R, our sphere-plus-cavity model gives a good description of the interaction of a single atom with molecules or intermediate-size spherical clusters of atoms. Note that in this case the potential explicitly depends on both the sphere and cavity radii. The theory could be applied (e.g., in cell biology) to study the vdW-force-induced transfer of an atom or a very small molecule from one cell into another, where it is attracted to another bigger (spherical) cell component or molecule. Note that local-field effects are automatically included.

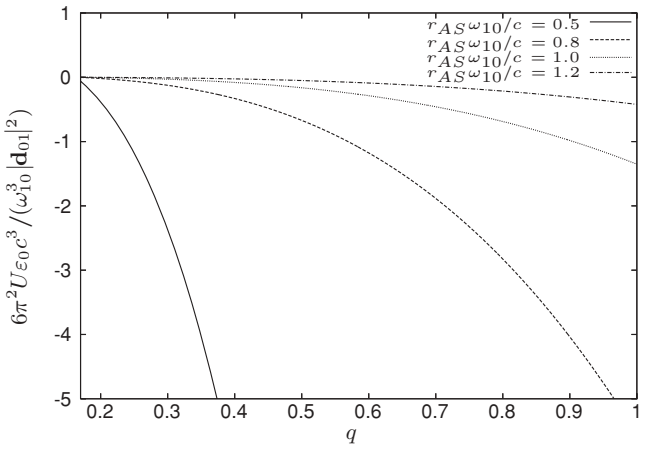

FIG. 3. CP potential $U(r_{AS})$ of a nonmagnetic atom in front of a dielectric sphere in an empty cavity embedded in bulk material vs. $q = R/R_C$ for different atom-sphere separations, $r_{AS}\omega_{10}/c$. Other parameters are $\omega_T/\omega_{10} = 1.03$, $\omega_{TS}/\omega_{10} = 1.0$, $\omega_{PS}/\omega_{10} = 6.0$, $\omega_P/\omega_{10} = 0.1$, and $\gamma_{(S)}/\omega_{10} = 0.001$.

As an example, let us consider the CP interaction of a nonmagnetic atom with a purely electric sphere (U_{ee}) in a bulk medium ($\varepsilon_\odot = \varepsilon_A = \varepsilon$). By substituting the required Green tensor (19) into Eq. (42), one easily finds

$$U(\mathbf{r}_A, \mathbf{r}_S) = -\frac{\hbar}{16\pi^3\varepsilon_0^2 r_{AS}^6}\int_0^\infty \mathrm{d}\xi \left[\frac{3\varepsilon(i\xi)}{2\varepsilon(i\xi)+1}\right]^2 \times \alpha_A(i\xi)\varepsilon(i\xi)\alpha^{\star}_{S+C}(i\xi)g[\sqrt{\varepsilon(i\xi)}\xi r_{AS}/c] \tag{54}$$

($r_{AS} = |\mathbf{r}_A - \mathbf{r}_S|$) with

$$g(x) = e^{-2x}(3+6x+5x^2+2x^3+x^4). \tag{55}$$

Figure 3 shows this potential for a two-level atom as a function of the relative sphere radius $q = R/R_C$ for various atom-sphere separations. We have used single-resonance models for the permittivities of the sphere and the medium:

$$\varepsilon_{(S)}(\omega) = 1 + \frac{\omega^2_{P(S)}}{\omega^2_{T(S)} - \omega^2 - i\omega\gamma_{(S)}}. \tag{56}$$

In Fig. 4, we show the potential U_{ee} as a function of the atom-sphere separation for different relative sphere radii $q = R/R_C$. Both figures show that for the constant ε_S considered here, larger spheres with their corresponding larger polarizabilities lead to stronger vdW attraction between the atom and the sphere.

III. SUMMARY AND CONCLUSIONS

We have studied the CP interaction of an atom with a small magnetodielectric sphere in an arbitrary magnetoelectric environment. By employing a point-scattering technique, we were able to express the Green tensor in the presence of the sphere as a simple function of the Green tensor of the environment. Using this result, we have found closed general expressions for the CP potential of a magnetoelectric atom interacting with a small magnetodielectric sphere, which depend on the sphere's polarizability and magnetizability.

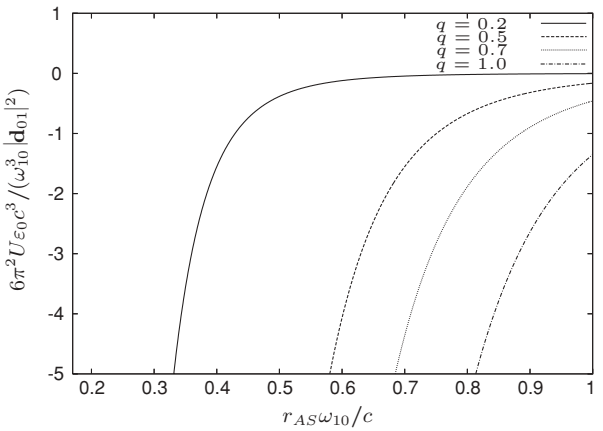

FIG. 4. $U(r_{AS})$ vs. $r_{AS}\omega_{10}/c$ for different ratios q. Other parameters are the same as in Fig. 3.

A comparison with the vdW potential between two ground-state atoms in the presence of the background medium has revealed how the different macroscopic and microscopic natures of atom versus sphere manifest themselves in the dispersion potentials: the immediate contact of a macroscopic sphere with the surrounding medium leads to the appearance of the permittivity and inverse permeability of the medium, whereas the coupling of the local electromagnetic field to the microscopic atom gives rise to local-field correction factors.

In order to interpolate between these two limiting cases, we have studied the potential of an atom with a sphere of variable radius located inside an Onsager cavity. The cavity represents the interspace between the particles contained in the sphere and those constituting the surrounding medium, so that our model can be used to study molecular systems of arbitrary size. Using similar techniques, we have derived the potential of an atom interacting with the sphere-plus-cavity system. We have shown that our result reduces to the atom-sphere or atom-atom potentials in the two limiting cases, in which the sphere radius is either much smaller than or equal to the cavity radius. As an example, we have considered the CP interaction between an electric atom and such a sphere-plus-cavity system, finding that the attractive potential diminishes as the sphere becomes smaller at a fixed cavity radius.

Our point-scattering method can also be used to calculate the Casimir force on a small sphere in an arbitrary environment and, in particular, the Casimir force between two small spheres. This problem will be subject of future work. A similar approach could be applied to dispersion interactions involving thin cylinders.

ACKNOWLEDGMENTS

This work was supported by the UK Engineering and Physical Sciences Research Council and the European Science Foundation Research Network CASIMIR. SYB is grateful for support by the Alexander von Humboldt Foundation.

[1] H. Margenau and N. R. Kestner, *Theory of Intermolecular Forces* (Pergamon Press, Oxford, 1969).
[2] J. Mahanty and B. W. Ninham, *Dispersion Forces* (Academic Press, London, 1976).
[3] G. Feinberg, J. Sucher, and C. K. Au, Phys. Rep. **180**, 83 (1989).
[4] P. W. Milonni, *The Quantum Vacuum* (Academic Press, New York, 1994).
[5] G. Compagno, R. Passante, and F. Persico, *Atom-Field Interactions and Dressed Atoms* (Cambridge University Press, Cambridge, 1995).
[6] V. A. Parsegian, *Van der Waals Forces: A Handbook for Biologists, Chemists, Engineers, and Physicists* (Cambridge University Press, New York, 2005).
[7] S. Y. Buhmann and D.-G. Welsch, Prog. Quantum Electron. **31**, 51 (2007).
[8] A. Salam, Int. Rev. Phys. Chem. **27**, 405 (2008).
[9] S. Scheel and S. Y. Buhmann, Acta Phys. Slovaka **58**, 675 (2008).
[10] M. B. Bordag, G. L. Klimchitskaya, U. Mohideen, and V. M. Mostepanenko, *Advances in the Casimir Effect* (Oxford University Press, Oxford, 2009).
[11] J. D. van der Waals, Ph.D. thesis, Universiteit Leiden, Leiden, 1873.
[12] F. London, Z. Phys. **63**, 245 (1930).
[13] H. B. G. Casimir and D. Polder, Phys. Rev. **73**, 360 (1948).
[14] A. Lambrecht, Phys. World **15**, 29 (2002).
[15] S. M. Gatica, M. W. Cole, and D. Velegol, Nano Lett. **5**, 169 (2005).
[16] H.-Y. Kim, J. O. Sofo, D. Velegol, M. W. Cole, and A. A. Lucas, Langmuir **23**, 1735 (2007).
[17] D. N. Thomas, S. J. Judd, and N. Fawcett, Water Res. **33**, 1579 (1999).
[18] J. W. Liu and E. Luijten, Phys. Rev. Lett. **93**, 247802 (2004).
[19] A. W. Rodriguez, J. N. Munday, J. D. Joannopoulos, F. Capasso, D. A. R. Dalvit, and S. G. Johnson, Phys. Rev. Lett. **101**, 190404 (2008).
[20] C. Hertlein, L. Helden, A. Gambassi, S. Dietrich, and C. Bechinger, Nature **451**, 172 (2008).
[21] J. Gregory, Water Sci. Technol. **27**, 1 (1993).
[22] Y. Liang, N. Hilal, P. Langston, and V. Starov, Adv. Colloid Interface Sci. **134–135**, 151 (2007).
[23] M. Fuchs and K. Schweizer, J. Phys. C: Condens. Matter. **14**, R239 (2002).
[24] V. A. Parsegian, A. Rev. Biophys. Bioeng. **2**, 221 (1973).
[25] J. N. Israelachvili, *Intermolecular and Surface Forces* (Academic Press, New York, 1991).
[26] M. V. Volkenstein, *Molecular Biophysics* (Academic Press, New York, 1977).
[27] J. N. Israelachvili, Q. Rev. Biophys. **6**, 341 (1974).
[28] S. Nir, Prog. Surf. Sci. **8**, 1 (1977).
[29] L. W. Bruch, Phys. Rev. B **72**, 033410 (2005).
[30] F. London, Trans. Faraday Soc. **33**, 8 (1937).
[31] H.-Y. Kim, J. O. Sofo, D. Velegol, M. W. Cole, and G. Mukhopadhyay, Phys. Rev. A **72**, 053201 (2005).
[32] H. Hamaker, Physica **4**, 1058 (1937).

[33] E. M. Lifshitz, Sov. Phys.—JETP **2** (1956).
[34] I. Dzyaloshinskii, E. M. Lifshitz, and L. Pitaevskii, Adv. Phys. **10**, 165 (1961).
[35] L. Onsager, J. Am. Chem. Soc. **58**, 1486 (1936).
[36] Ho Trung Dung, S. Y. Buhmann, and D.-G. Welsch, Phys. Rev. A **74**, 023803 (2006).
[37] A. Sambale, S. Y. Buhmann, D.-G. Welsch, and M. S. Tomaš, Phys. Rev. A **75**, 042109 (2007).
[38] R. Messina, D. A. R. Dalvit, P. A. M. Neto, A. Lambrecht, and S. Reynaud, Phys. Rev. A **80**, 022119 (2009).
[39] S. Y. Buhmann, Ho Trung Dung, and D.-G. Welsch, J. Opt. B: Quantum Semiclass. Opt. **6**, S127 (2004); J. Phys. B **39**, 3145(E) (2006).
[40] M. M. Taddei, T. N. C. Mendes, and C. Farina, e-print arXiv:0903.2091 (2009).
[41] M. Boustimi, J. Baudon, J. Robert, A. Semlali, and B. Labani, Phys. Rev. B **62**, 7593 (2000).
[42] H. Safari, D.-G. Welsch, S. Y. Buhmann, and S. Scheel, Phys. Rev. A **78**, 062901 (2008).
[43] L.-W. Li, P.-S. Kooi, M.-S. Leong, and T.-S. Yeo, IEEE Trans. Microwave Theory Tech. **42**, 2302 (1994).
[44] W. C. Chew, *Waves and Fields in Inhomogeneous Media* (IEEE Press, New York, 1995).
[45] S. Y. Buhmann and D.-G. Welsch, Appl. Phys. B **82**, 189 (2006).
[46] M. Xu and M. J. Dignam, J. Chem. Phys. **96**, 3370 (1992).
[47] L. D. Landau and E. M. Lifshitz, *Electrodynamics of Continuous Media*, 2nd ed. (Pergamon Press, Oxford, 1984), Vol. 8.
[48] A. D. McLachlan, Discuss. Faraday Soc. **40**, 239 (1965).
[49] S. Y. Buhmann and S. Scheel, Phys. Rev. Lett. **102**, 140404 (2009).
[50] S. Y. Buhmann and S. Scheel, Int. J. Mod. Phys. A **24**, 1796 (2009).
[51] J. D. Jackson, *Classical Electrodynamics*, 3rd ed. (Wiley, New York, 1998).